Magneto-optical optimization of magnetic microwires for GMI sensors

A. Chizhik[1]*, A. Zhukov[1,2,3]

[1]Dpto. Fisica de Materiales, Facultad de Quimica, Universidad del País Vasco UPV/EHU, San Sebastian, Spain

[2]Department Applied Physics I, EUPDS, UPV/EHU, 20018, San Sebastian, Spain

[3]IKERBASQUE, Basque Foundation for Science, Bilbao, Spain

*oleksandr.chyzhyk@ehu.es

P. Gawronski

AGH University of Krakow, Poland

OUTLINE

Introduction

Experimental technique

Experimental results

Conclusions

Introduction

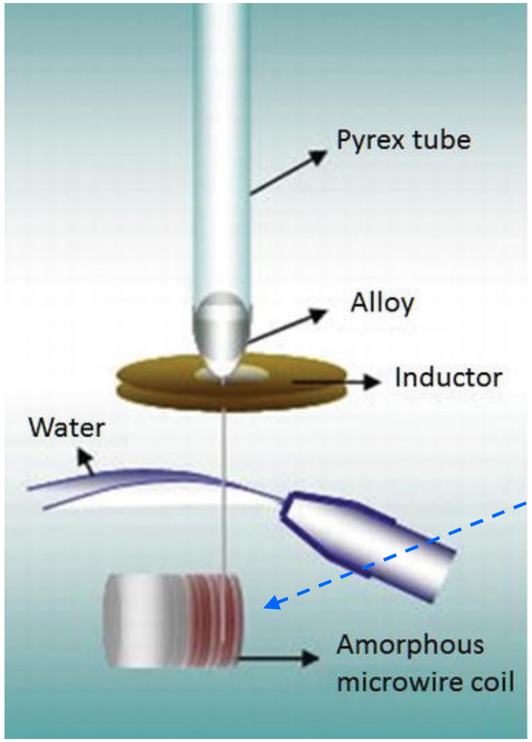

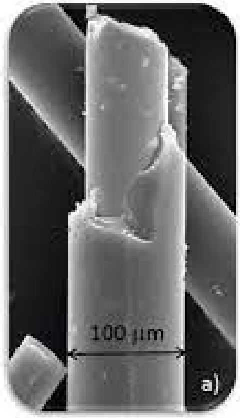

Amorphous cylindrical magnetic microwires with metallic nucleus

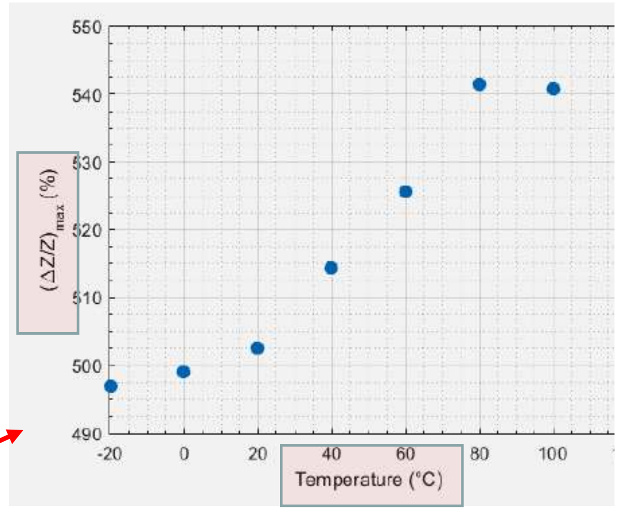

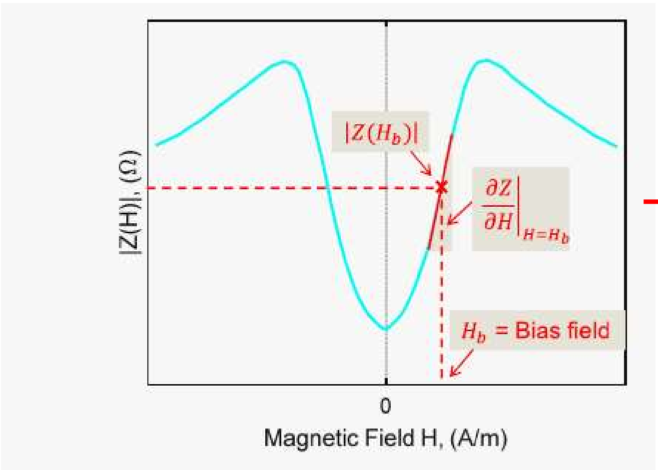

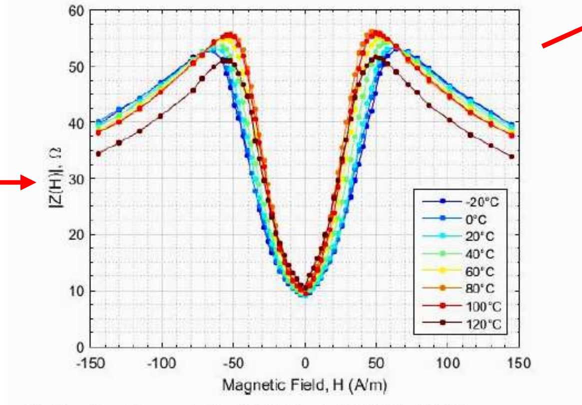

Temperature Dependence of Giant Magnetoimpedance in Amorphous Microwires for Sensor Application J. Nabias, A. Asfour, J. Yonnet 2017 Materials Science IEEE Transactions on Magnetics

Introduction

glass covered wire

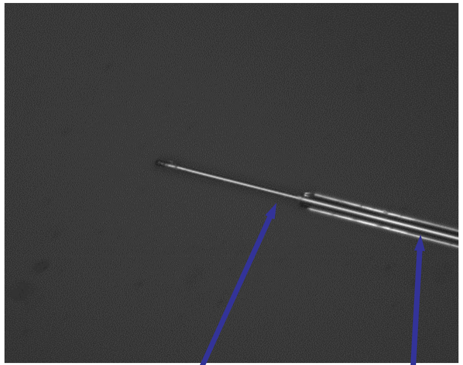

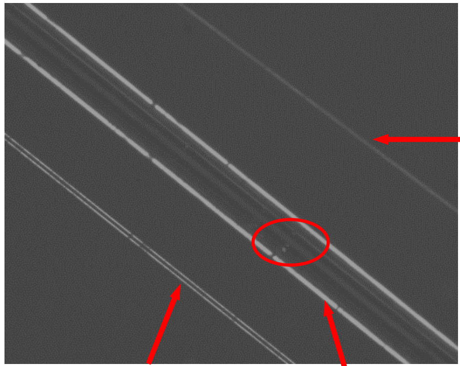

metallic nucleus | glass covering

1 μm

10 μm

100 μm

MHz-GHz

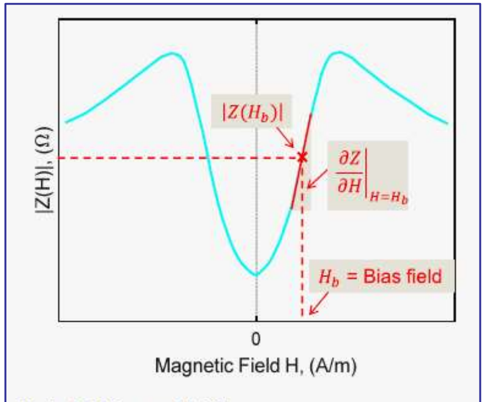

Typical GMI curve $|Z(H)|$.

Giant Magneto-Impedance (GMI) effect

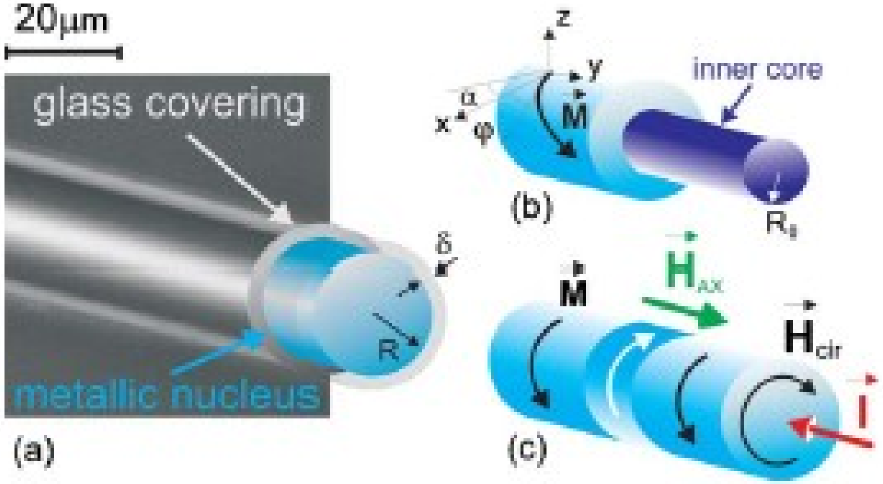

AICHI STEEL CORPORATION

Electronic compass in C7-00

3-Axis

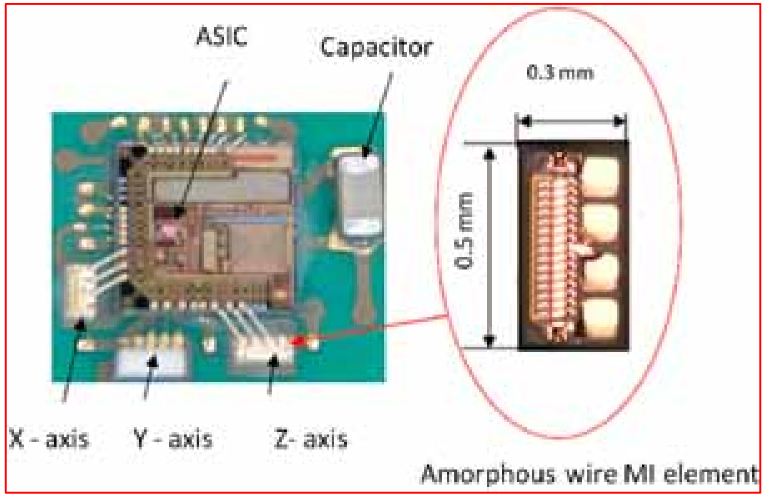

One of the features of soft magnetic materials quite relevant for magnetic sensors and devices is so-called giant magnetoimpedance (GMI). The origin of the GMI effect as well as the main characteristics of GMI are satisfactorily explained in terms of classical electrodynamics, taking into account the skin effect of a soft magnetic conductor. High magnetic permeability of amorphous magnetic materials is a prerequisite for the implementation of the GMI effect.

$$\delta = \sqrt{\frac{c^2}{2\pi\Omega\omega\mu}}$$

$$Z \sim (\mu\Omega)^{-1/2}$$

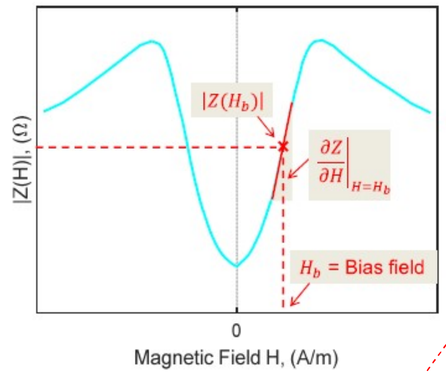

Fig. 1. Typical GMI curve $|Z(H)|$.

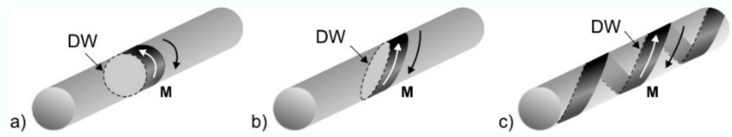

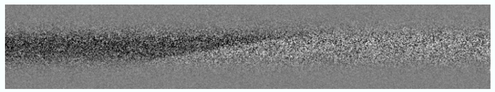

JOURNAL OF APPLIED PHYSICS **109**, 113924 (2011)

Correlation of surface domain structure and magneto-impedance in amorphous microwires

M. Ipatov,[1,a)] A. Chizhik,[1] V. Zhukova,[1] J. Gonzalez,[1] and A. Zhukov[1,2]
[1]*Department de Física de Materiales, Universidad del País Vasco, San Sebastián, Spain*
[2]*IKERBASQUE, Basque Foundation for Science, 48011 Bilbao, Spain*

Magnetic microwires with longitudinally distributed magnetic properties

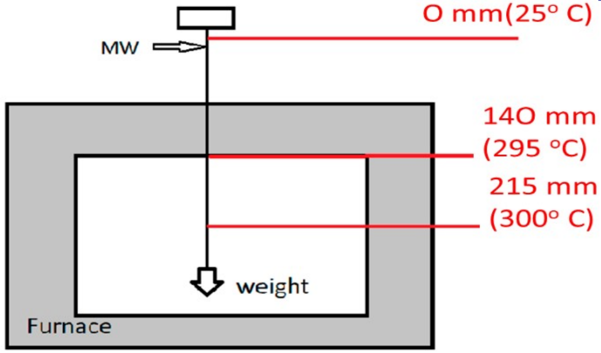

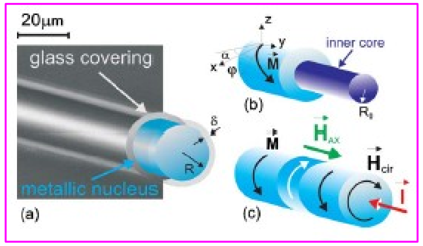

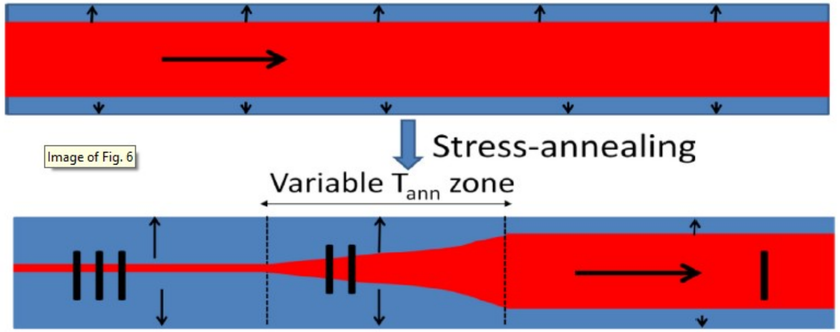

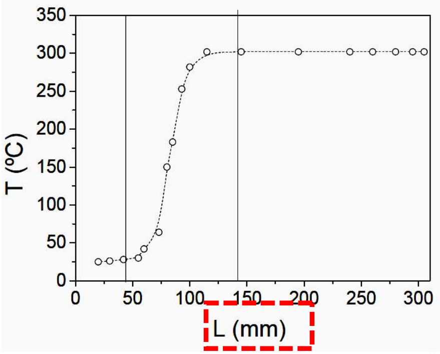

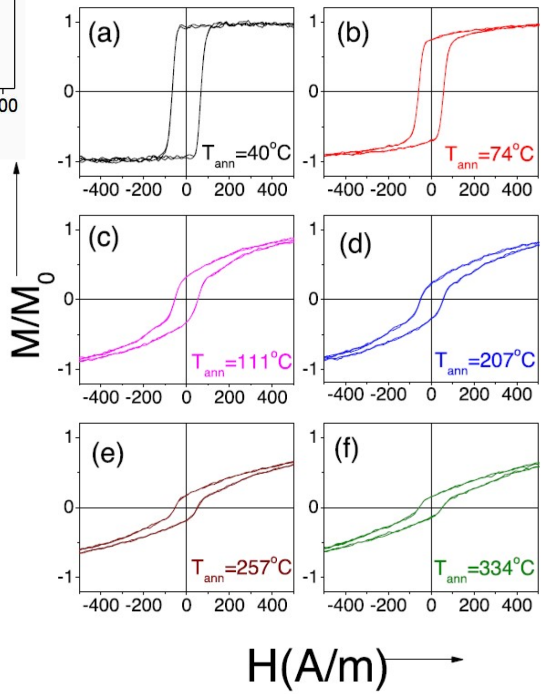

ɡ. 3. Hysteresis loops of $Fe_{75}B_9Si_{12}C_4$ microwires stress-annealed at variable
easured by short pick-up coil.

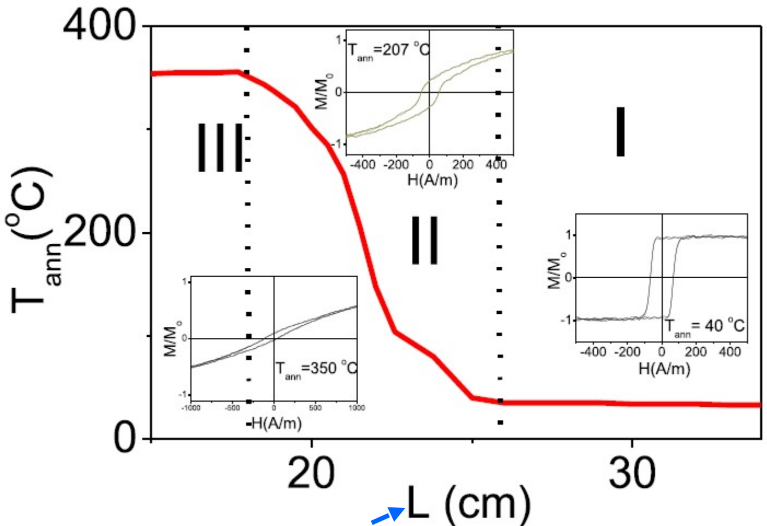

Schematic picture of the graded magnetic anisotropy appearing as a continuous magnetic anisotropy gradient over the microwire length obtained by stress-annealing at variable *T ann* .

Engineering of domain wall propagation in magnetic microwires with graded magnetic anisotropy

P. Corte-León[a,b], V. Zhukova[a,b], J.M. Blanco[b], A. Chizhik[a], M. Ipatov[a,b], J. Gonzalez[a], A. Fert[a,c], A. Alonso[d], A. Zhukov[a,b,e,*]

Applied Materials Today 26 (2022) 101263

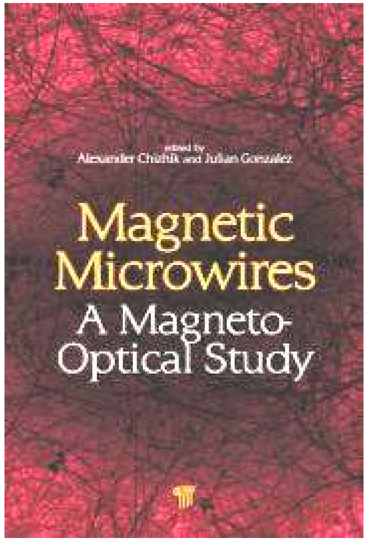

Alexander Chizhik and Julian Gonzalez
Book "Magnetic Microwires. A Magneto-Optical Study"

Pan Stanford Publishing 2014

A. Stupakiewicz, A. Chizhik, M. Tekielak,
A. Zhukov, J. Gonzalez, and A. Maziewski
Direct imaging of the magnetization
reversal in microwires using all-MOKE microscopy
Review of Scientific Instruments 85, 103702 (2014)

A. Chizhik, A. Zhukov, J. Gonzalez, P. Gawroński,
K. Kułakowski & A. Stupakiewicz,
Spiral magnetic domain structure in
cylindrically-shaped microwires
Scientific reports (2018) 8:15090

MOKE experiment

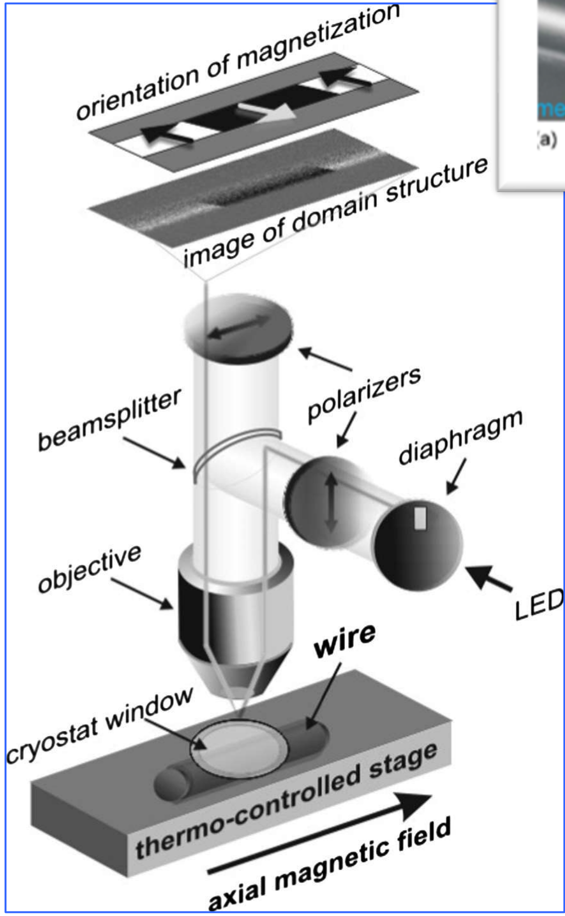

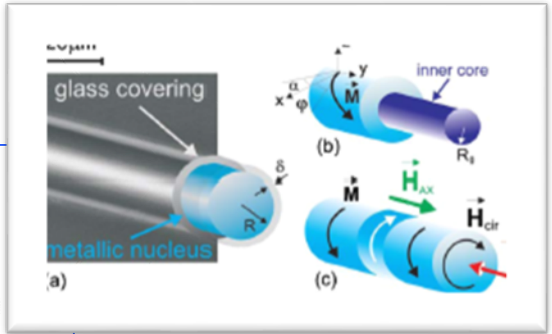

Schematic configuration of MOKE microscopy for the observation of the magnetic domain structures in microwires.

Experimental technique

magneto-optical Kerr effect (MOKE)

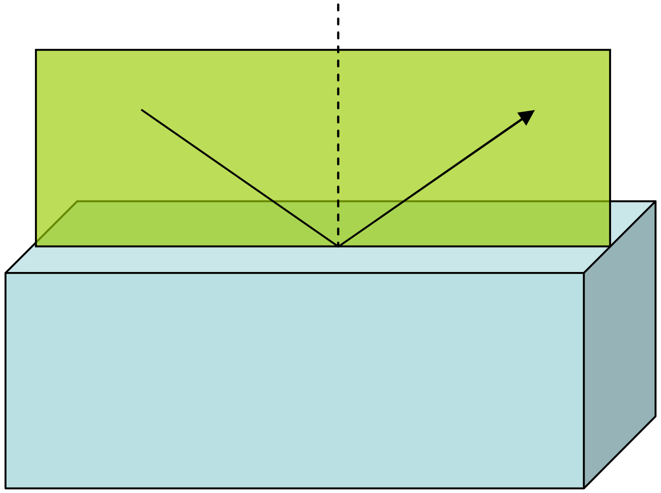

Traditional MOKE

MOKE of cilindrically shaped wires

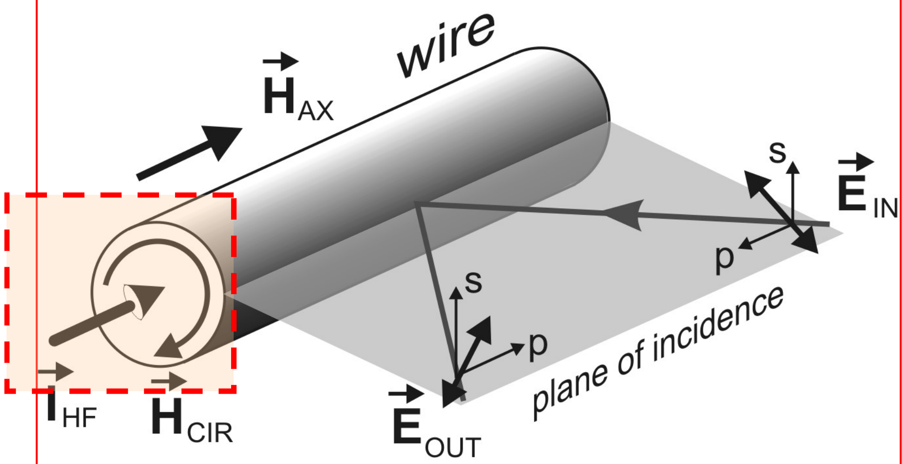

Variety of surface domain structures

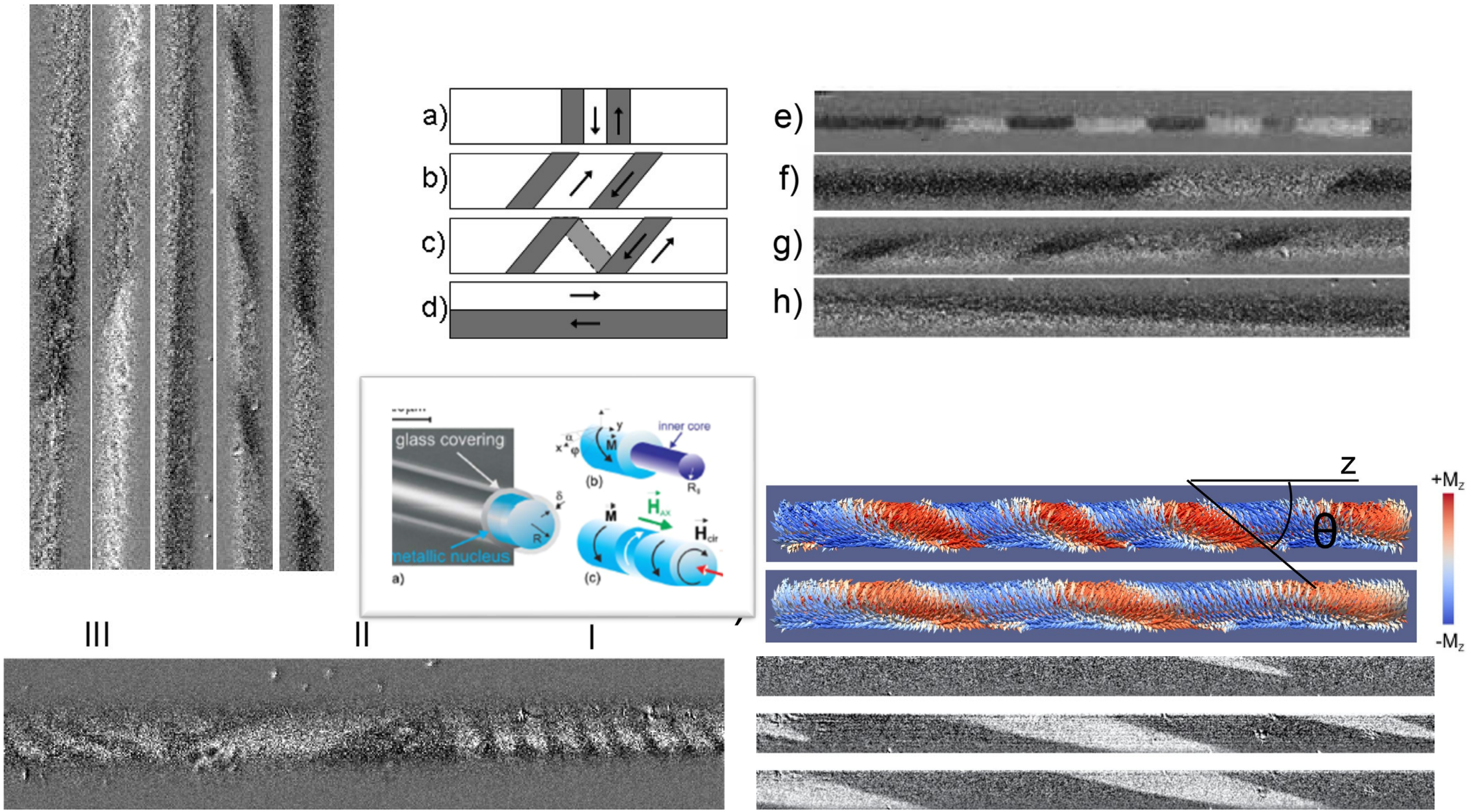

EXPERIMENT

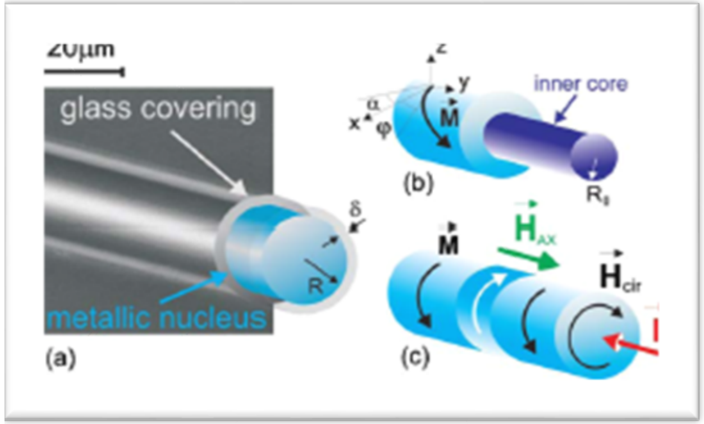

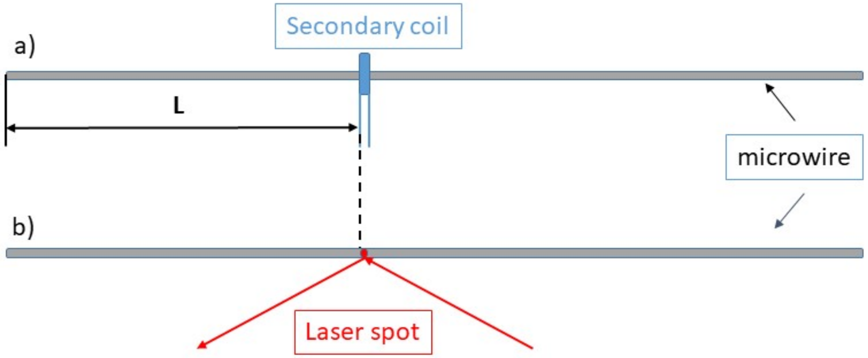

Schematic picture of a) magnetic and b) MOKE experiments.
L is the distance from the end of the microwire to the point of measurement

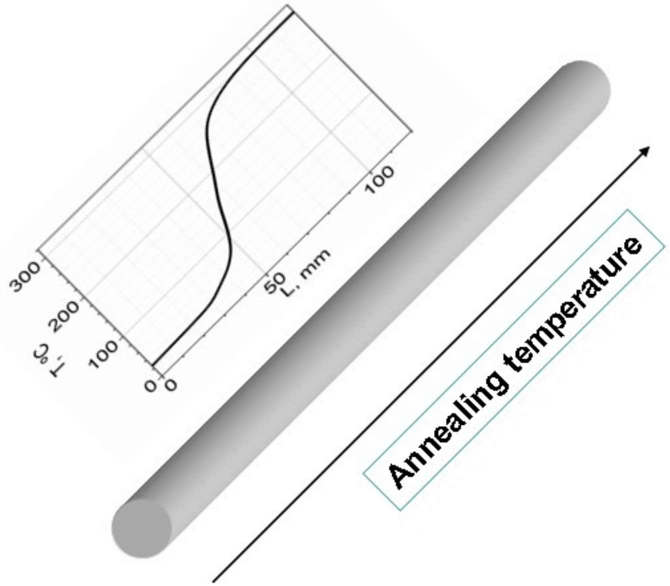

We studied glass-coated microwire with chemical composition of $Co_{64.04}Fe_{5.71}B_{15.88}Si_{10.94}Cr_{3.4}Ni_{0.3}$ (diameter of metallic nucleus d=94 μm, total diameter with glass covering D=126 μm) prepared by Taylor-Ulitovsky technique. The long sample was manufactured to ensure a uniform distribution of magnetic properties along the microwire length. The homogeneous microwire was subjected to the annealing at variable temperature to obtain the microwire sample with **magnetic properties distributed along the microwire length.**

EXPERIMENT

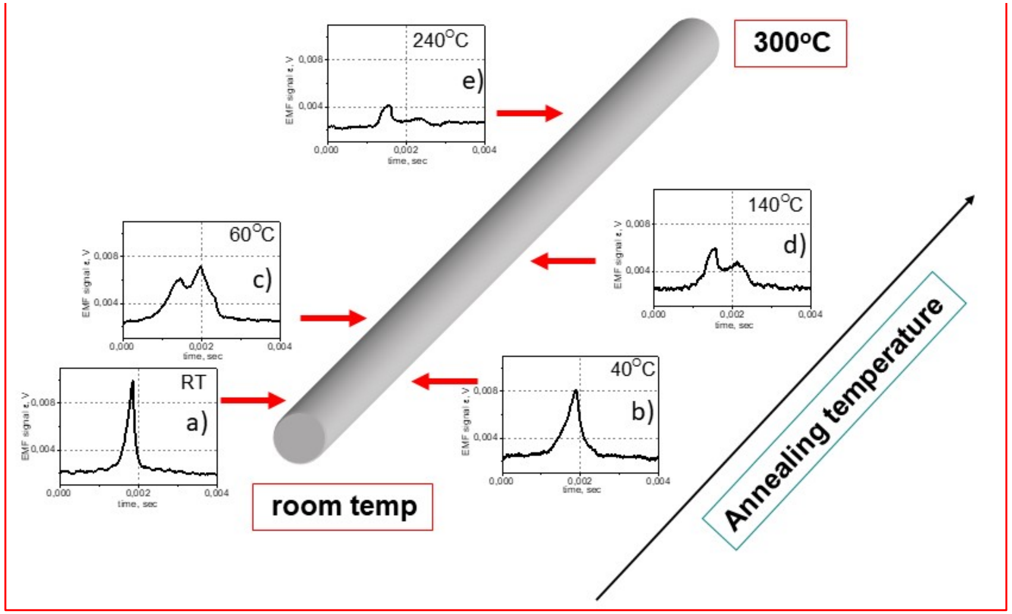

1) Distribution of *EMF* peak along the sample length.

Figure presents the *EMF* peak transformation obtained from one of the pick-up coils when the sample moves inside the measuring system. Other words, the transformation of the *EMF* peak with the annealing temperature is observed. Specifically, we have observed that starting from room temperature, as the annealing temperature increases, the shape of the peak changes significantly: the peak width increases, and the peak amplitude decreases until the peak disappears. In general terms, this means that the velocity associated with the passage of the DW along the pick-up coil decreases, while the width of the DW probably increases.

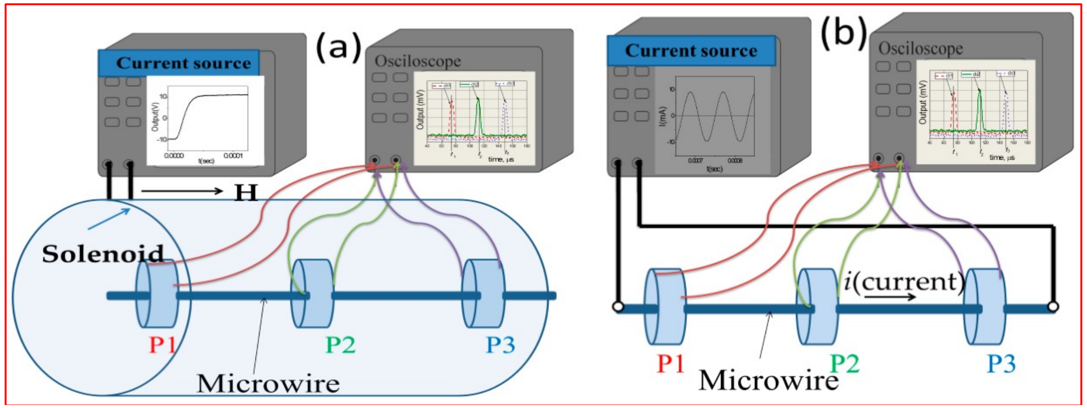

Method of Sixtus-Tonks

Schematic picture of the experimental set-up for measurements of magnetic field driven (**a**) and current driven (**b**) DW dynamics in microwires.

EXPERIMENT

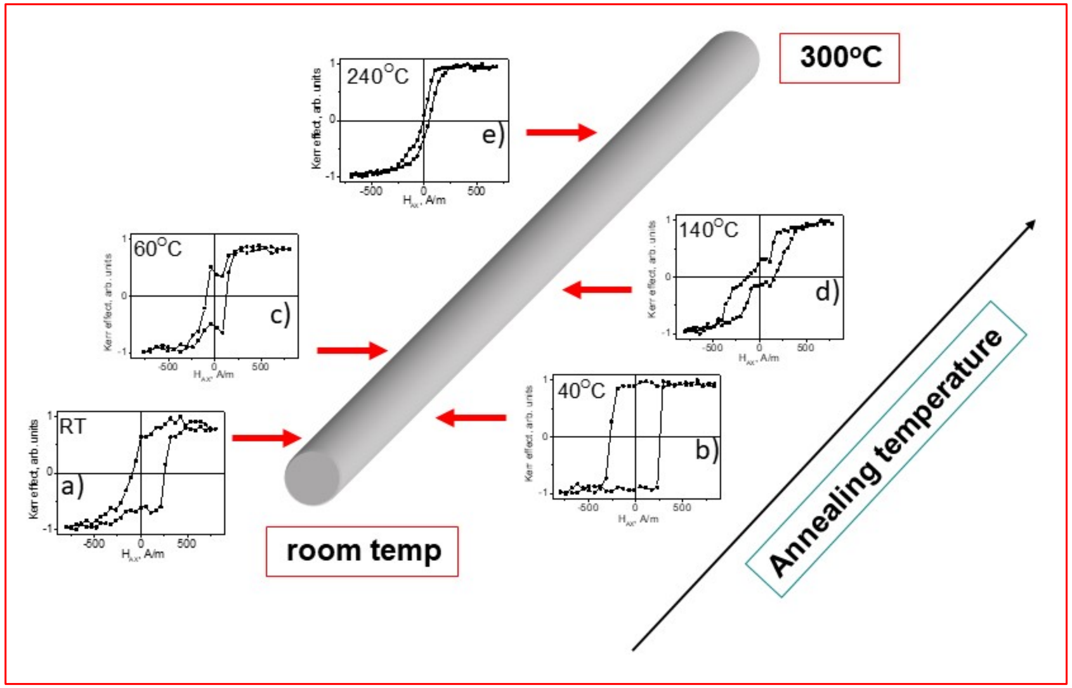

2) Distribution of MOKE hysteresis loops along the sample length

Figure demonstrate the **local MOKE hysteresis loops** obtained in different places on the surface of the long sample annealed at different temperature. Moving along the sample from the room temperature upwards, we found the noticeable transformation of the MOKE hysteresis loop. There is a certain correlation between the results presented in the figures. Although this correlation is not obvious at first glance, we will demonstrate it during the comparative analysis of the obtained results. A certain asymmetry of the hysteresis curves is observed at RT and 40^{O}C, while at temperatures of 60^{O}C, 140^{O}C and 240^{O}C they are symmetrical enough. **Being rectangular or nearly rectangular at temperatures close to room temperature, the MOKE hysteresis curves become progressively flatter as we move along the long sample towards the locations corresponding to higher temperatures of the annealing.**

EXPERIMENT

ANALYSIS

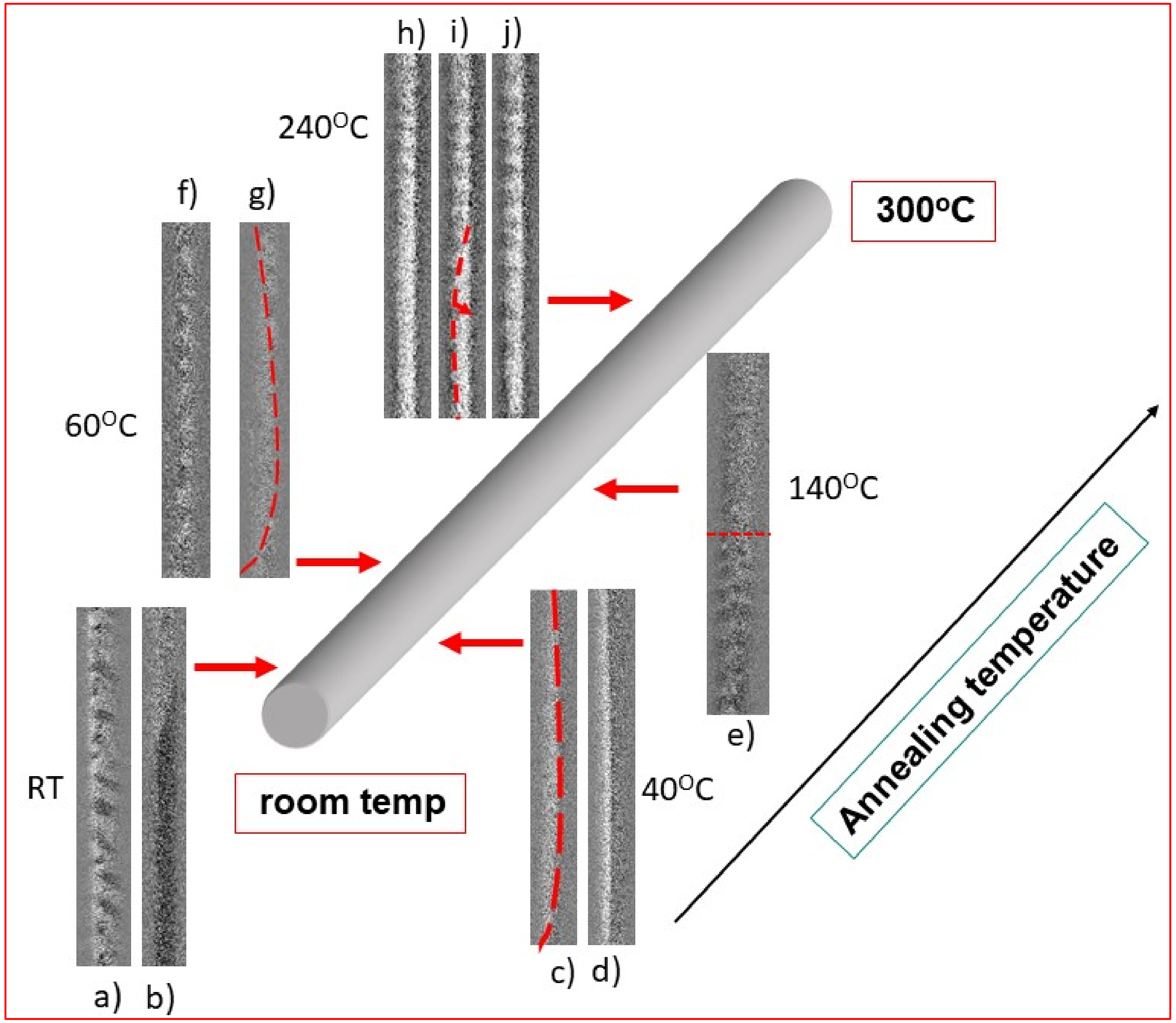

3) Distribution of surface domain structure along the sample length

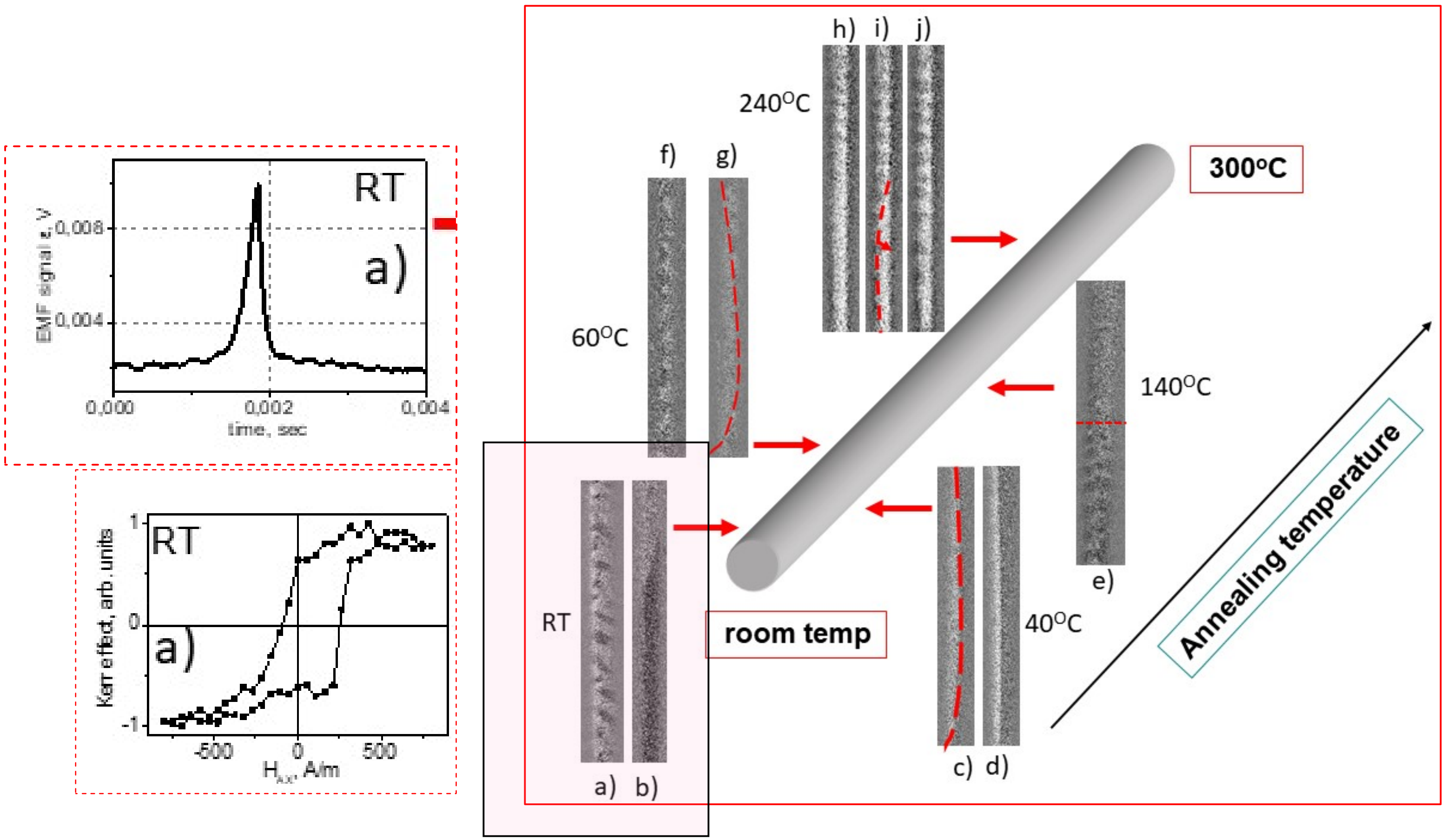

3) Distribution of surface domain structure along the sample length

a) Room temperature. Here we have determined that the image b corresponds to the sharp jump in the MOKE hysteresis (right semi-loop of the Fig. a), while the image a corresponds to the relatively slow magnetization reversal in the same MOKE hysteresis curve. The Fig. b is the evidence that the magnetization reversal occurs as the fast motion of the inclined elliptic domain wall. The Fig. a reflects a relatively slow formation and the transformation of the multi-domain structure.

ANALYSIS

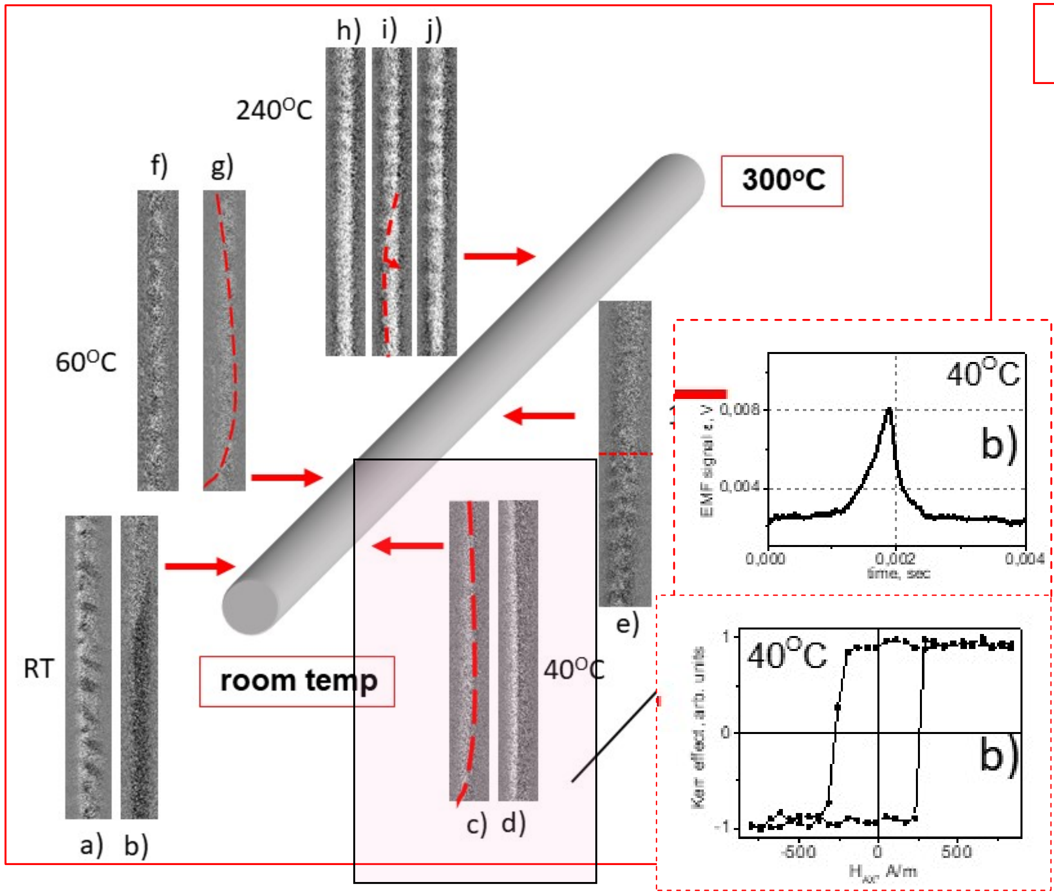

Distribution of surface domain structure along the sample length

b) Temperature of 40º. At this temperature, we also observe two different domain structures corresponding to two semi-loops (Fig. b). The very sharp jump (right semi-loop of the Fig. b) is associated with quick motion of the longitudinally oriented DW (Fig. d). On the reverse side of the MOKE loop, the motion of the long curved, almost linear DW is observed (Fig. c). This DW we qualified as the variation of the long spiral DW observed earlier.

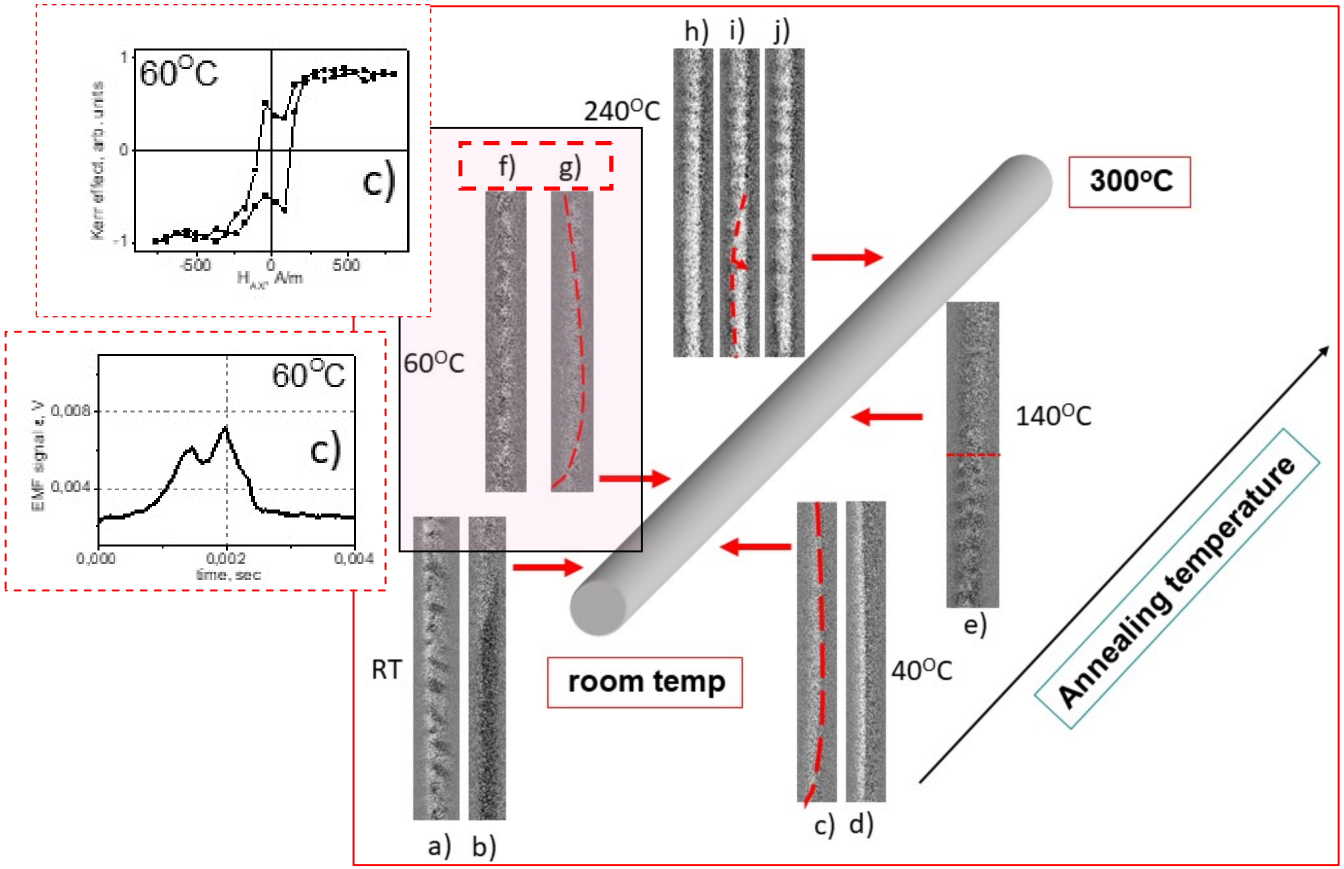

ANALYSIS

Distribution of surface domain structure along the sample length

c) For the location in the surface of the sample corresponding to the **annealing temperature of 60º**, the MOKE hysteresis loop is symmetrical (Fig. **c**). This means that the magnetization reversal occurred in similar ways when the external magnetic field was reversed. Figures **f** and **g** correspond to this process of the magnetization reversal. This process consists of two stages. At the first stage, the low formation and transformation of the multi-domain structure takes place (Fig. **f)**. At the second stage (sharp jump in the Fig. **c**) the rapid movement of the curved DW occurs (Fig. **g**). Visually, this is observed in such a way that the curved DW "washes away" the slow multi-domain structure formed earlier at the first stage of the magnetization reversal.

ANALYSIS

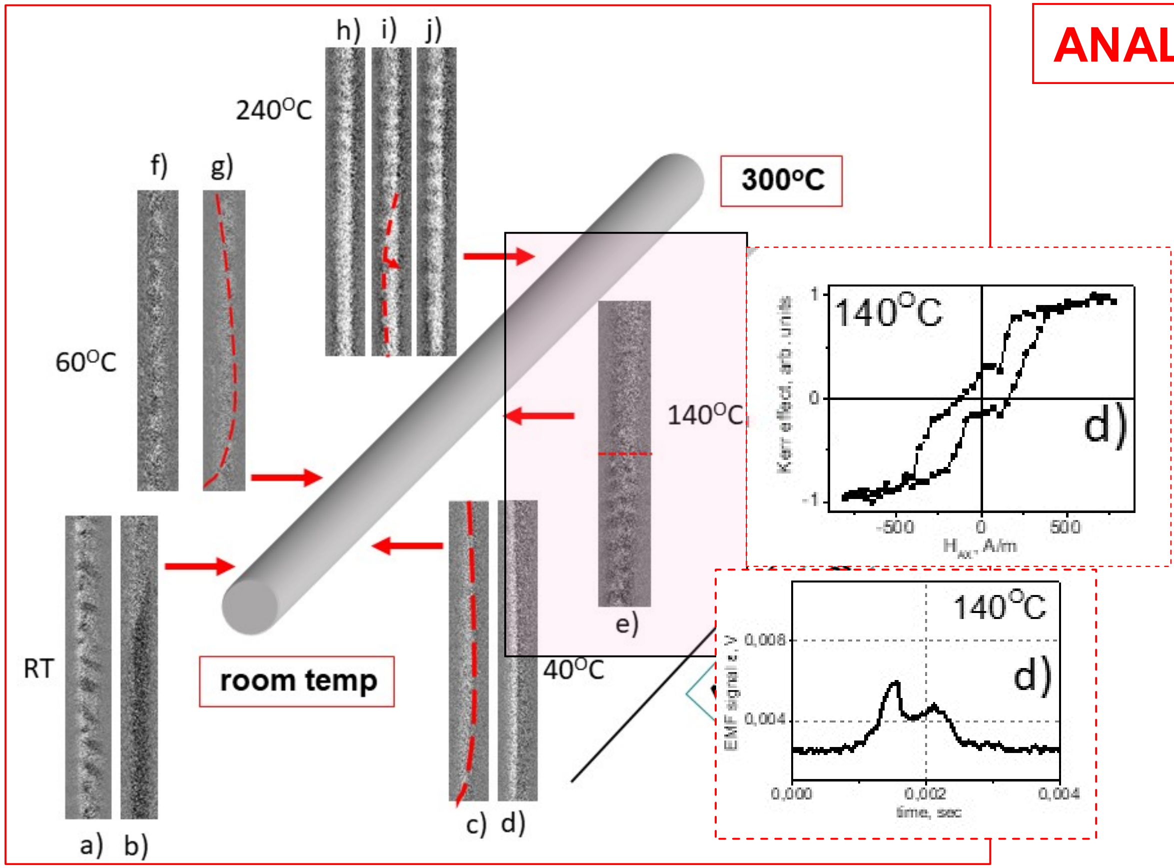

Distribution of surface domain structure along the sample length

d) The magnetization reversal process in the location corresponding to the **annealing temperature of 140º** is also a combination of two types of domain structure. We observed two processes that went on simultaneously, or succeeded one another. **The first process** is, as in the case of the 60º, the formation and slow transformation of the multi-domain structure placed almost perpendicularly to the microwire axis. The second process is the quick **jump-like motion of the circular DW** moving along the microwire surface. The presence of this type of jumps is probably associated with the presence of defects on the surface of the microwire adjacent to the glass coating.

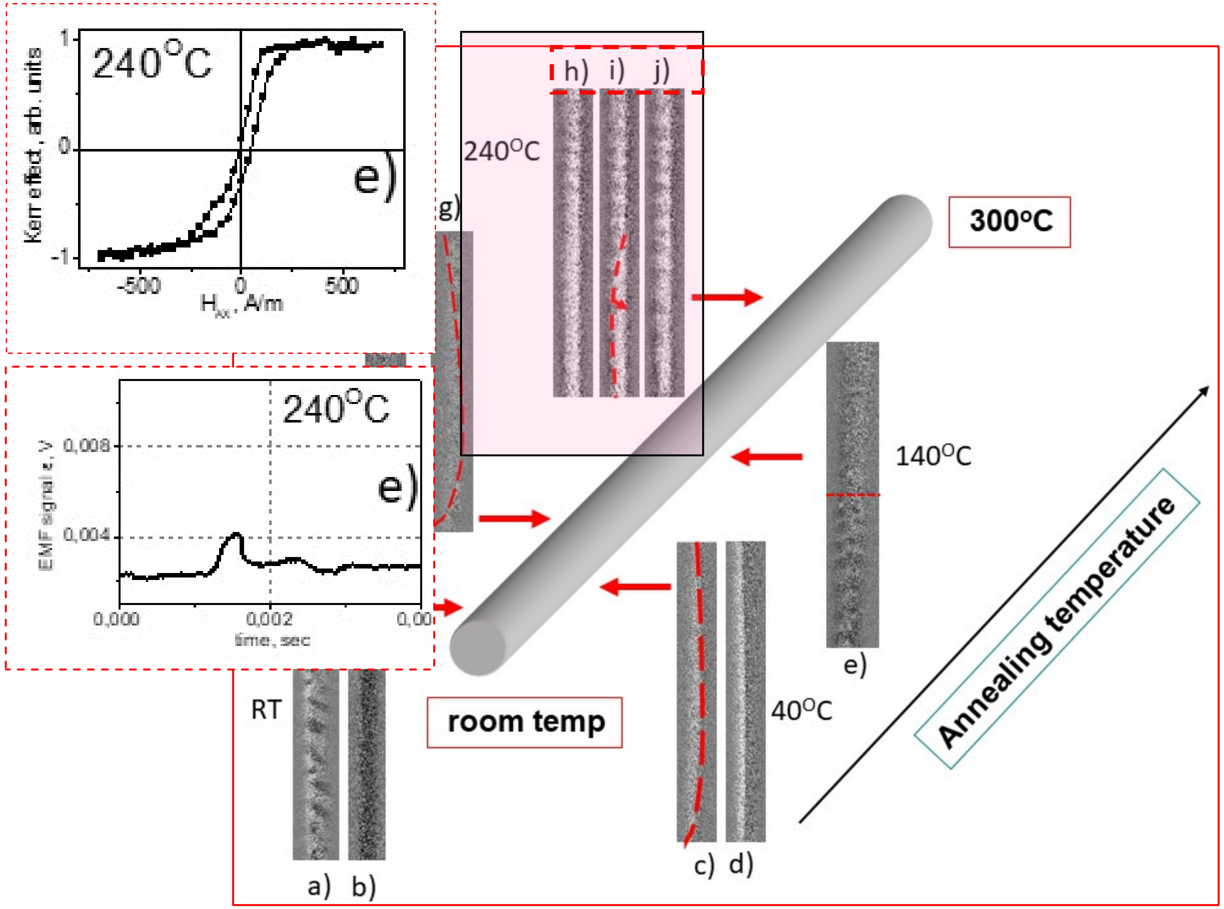

Distribution of surface domain structure along the sample length

e) Finally, in the location in the surface of the microwire corresponding to the **annealing temperature of 240º C** we have found the domain structure which could be tentatively named "slow spiral structure" which is characterized namely by the relatively low velocity of the motion along the microwire surface. Figures **h, i and j** demonstrate the consistent motion of slightly inclined spiral domains. The red dashed line shows the position of the **front** separating the mono-domain part from the part filled by the spiral structure. The arrow shows the direction of movement of this front. This slow movement corresponds to a smooth curve without jumps (Fig. e).

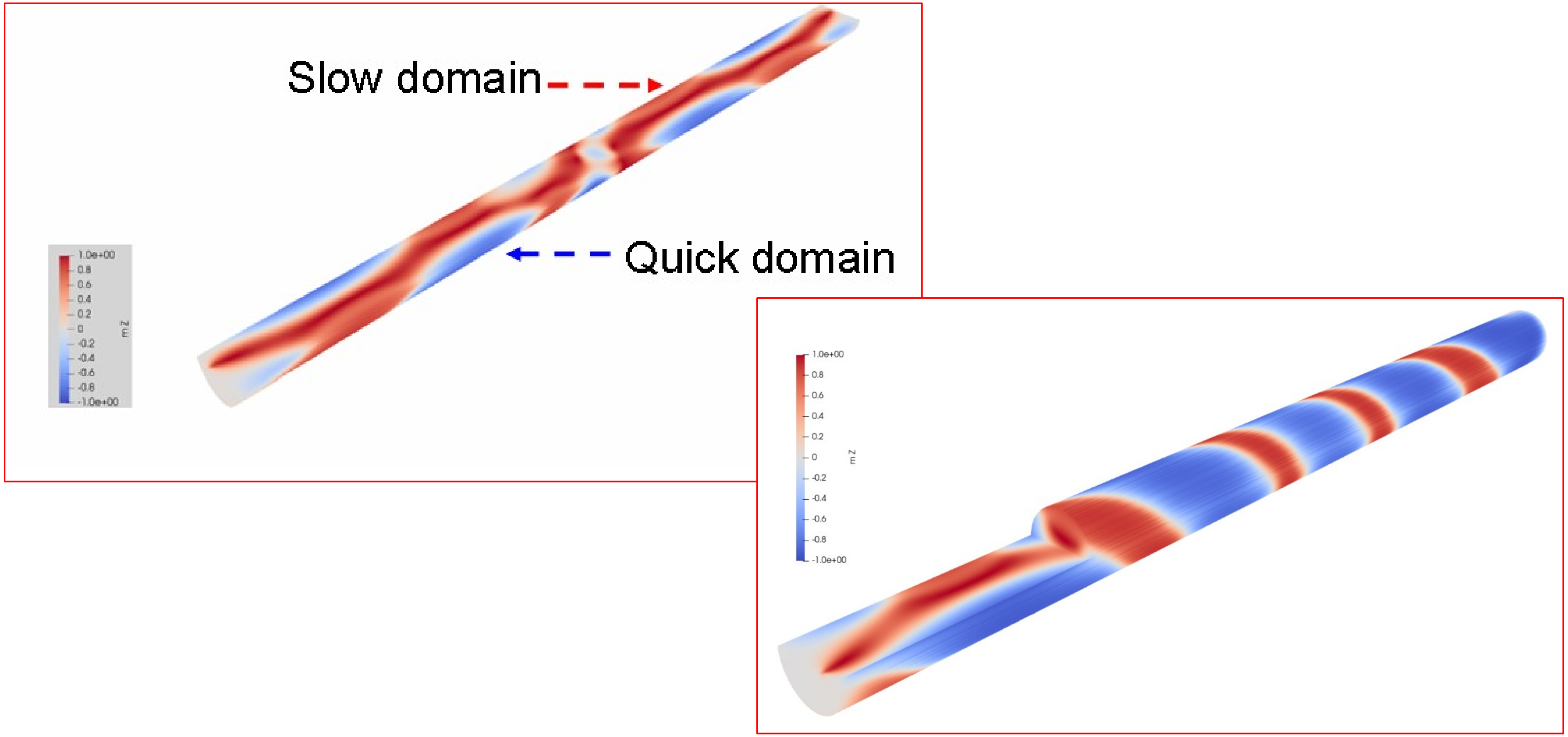

Calculated domain structure presented as half-tube

Figure shows the calculated domain structure on the flat surface of the semi-cylinder. It should be noted that initially the calculations were carried out for all points inside the whole cylinder, and the results are shown in the form of a semi-cylinder for clarity of the analysis. Red and blue colors correspond to two opposite axial direction of the magnetization. Here we also observe two types of domains: **red domains correlated with the internal part (modified inner core) and blue domains, independent form the inner domains.**

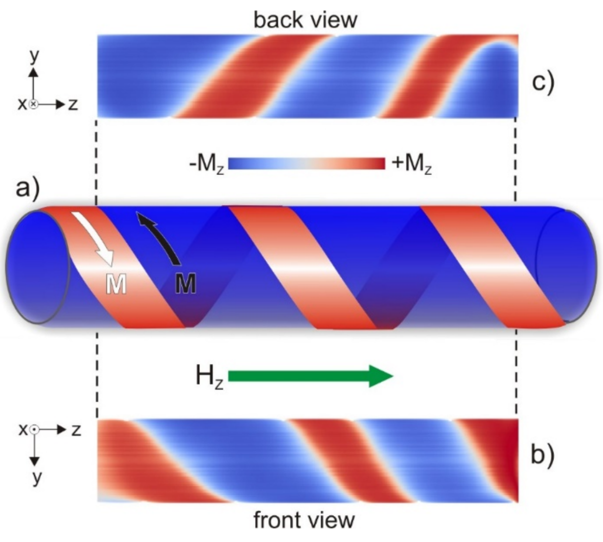

P. Gawronski, AGH University Krakow, Poland

Simulations. A theoretical analysis of the obtained results was performed on the basis of a model assuming that, for a magnetostrictive microwire, the cylindrical symmetry limits the stress components to radial (*srr*), circumferential (*sqq*) and axial (*szz*) components (i.e., a **different stress along each axis**). Further, the energy of the magnetic anisotropy is equivalent to the barrier energy necessary to rotate a local magnetic moment. **The magnetic anisotropy energy possesses a uniaxial character that is equivalent to the cylindrical symmetry of the angular dependence of the magnetic moment**. That is to say, for a local easy axis along the *OZ* direction, the energies needed to rotate the magnetic moment within the *ZX* plane and within the *ZY* plane are the same. **The concept of an effective uniaxial anisotropy, *Ku*, considers that the magnetic moment is rotated within the plane where the energy cost is lower.** Thus, if the circumferential, radial and axial magnetic moment components value as $\sigma qq < \sigma rr < \sigma zz$, then $Ku = (3/2)\lambda(\sigma zz - \sigma rr)$, where λ is the magnetostriction constant. Thus, the energy to rotate the magnetic moment in the *ZX* plane is less than that necessary to rotate it in the *ZY* plane. Micromagnetic modelling herein were performed using the MuMax3 simulation tool.

CONCLUSIONS

Our extensive research was aimed at the studying of the magnetic properties of microwires with distributed magnetic properties. These distributed properties were determined by the distribution of magnetic anisotropy, which in turn was determined by the process of annealing at variable temperature. In our opinion, the most significant result obtained is that we managed to recognize a wide variety of the complex magnetic structures in various longitudinal locations on the surface of the microwire.

We succeeded in determining the basic differences between these magnetic structures, which are manifested in the features of the magnetization reversal process. The complex use of the techniques allowed us to look at the problem from an unexpected angle and find those basic features of magnetic structures that were implemented in all the applied experimental techniques.

To the analysis of the obtained results, we involved the results of well-proven theoretical calculations. As we were able to establish, the investigated domain structures can be divided into two classes, which are characterized by the velocity of their transformation and motion. We determined that the reason for this is the different degree of coupling of surface domains with the internal domain structure. The combination of helical, elliptical, curved, axial and circular domain structures changes smoothly as the point of the observation moves along the microwire surface from room temperature to a maximum annealing temperature of 300 degrees.